Published in final edited form as:
Cancer Lett. 2011 December 1; 311(1): 57–65. doi:10.1016/j.canlet.2011.06.023.

Indole-3-carbinol inhibited tobacco smoke carcinogen-induced lung adenocarcinoma in A/J mice when administered during the post-initiation or progression phase of lung tumorigenesis

Xuemin Qian[1], **Tamene Melkamu**[2], **Pramod Upadhyaya**[1], and **Fekadu Kassie**[1,3]

[1]Masonic Cancer Center, University of Minnesota, Minnesota, USA

[2]Department of Animal Science, University of Minnesota, Minnesota, USA

[3]College of Veterinary Medicine, University of Minnesota, Minnesota, USA

Abstract

We studied the chemopreventive efficacy of indole-3-carbinol (I3C), a phytochemical found in cruciferous vegetables, to inhibit tobacco carcinogen-induced lung adenocarcinoma in A/J mice when given following post-initiation or progression protocol. Moreover, we assessed the potential mechanisms responsible for the anticancer effects of I3C. Post-initiation administration of I3C decreased the multiplicity of surface tumors as well as all forms of histopathological lesions, including adenocarcinoma, whereas administration of the compound during tumor progression failed to decrease the multiplicity of surface tumors and early forms of microscopic lesions but reduced the frequency of adenocarcinoma. Mechanistic studies in A549 lung adenocarcinoma cells indicated that the lung cancer preventive effects of I3C are mediated, at least in part, via modulation of the receptor tyrosine kinase/PI3K/Akt signaling pathway.

Keywords

chemoprevention; 4-(methylnitrosamino)-1-(3-pyridyl)-1-butanone; indole-3-carbinol; A549 cells; lung adenocarcinoma

1. Introduction

Accumulating data indicate an inverse relationship between consumption of cruciferous vegetables and the incidence of several cancers, including lung cancer [1–4]. These effects have been attributed to the presence in these vegetables of glucosinolates [5–7]. Upon hydrolysis by the plant enzyme myrosinase, glucosinolates give rise to isothiocyanates or indoles, depending on the type of glucosinolate. Generally, alkyl and aralkyl glucosinolates yield mainly isothiocyanates, whereas indolyl glucosinolates produce indole-3-carbinol (I3C) and related compounds [7]. Analysis of the glucosinolate content of commonly consumed cruciferous vegetables such as cabbage, broccoli, and cauliflower showed that indolyl glucosinolates account for 70–93% of the glucosinolates, indicating the importance of I3C and related compounds in the cancer preventive activities of these vegetables [8]. Once ingested, I3C is converted into more than 15 oligomeric products [9]. Of these

Requests for reprints: Fekadu Kassie, Masonic Cancer Center, University of Minnesota, Mayo Mail Code 806, 420 Delaware Street SE, Minneapolis, MN 55455, USA. Phone: 612-625-9637; Fax: 612-626-5135; kassi012@umn.edu.

Conflict of interest
The authors declare no conflict of interest

compounds, only the cancer preventive activities of DIM have been extensively investigated [10–12].

Considerable evidence from murine models of cancer shows that I3C inhibits tumorigenesis at several sites, including breast, lung, colon, cervix, liver, prostate, and skin [9,14]. Studies in *in vitro* models demonstrated that I3C exerts anticancer effects by inhibiting the formation of free radicals, shifting estrogen metabolism towards the less estrogenic metabolite 2-hydroxyestrone, inducing G1/S arrest of the cell cycle and apoptosis, and suppressing tumor cell migration, invasion and angiogenesis [9,14]. In clinical trials, I3C showed promising efficacy for the prevention of breast cancer and for the treatment of vulvar intraepithelial neoplasia and human papilloma virus-induced cervical cancer [15].

In our earlier reports [16,17], we showed inhibition by I3C of tobacco carcinogen- or vinyl carbamate-induced lung adenocarcinoma in mice when the compound was administered during the post-initiation period. Here, we further extended our study and examined the comparative lung cancer chemopreventive efficacy of the compound when given during the post-initiation phase or the progression phase of lung tumorigenesis. Also, we assessed, using protein microarrays, modulation by I3C of receptor tyrosine kinases, non-receptor tyrosine kinases, and apoptosis-related proteins in A549 human lung adenocarcinoma cells. Our results showed that I3C inhibited lung adenocarcinoma when given early or late in the carcinogenesis process by modulating proteins involved in cancer cell proliferation, survival, invasion and angiogenesis, in particular the receptor tyrosine kinase/PI3K/Akt signaling pathway.

2. Materials and Methods

2.1. Chemicals, reagents, and diets

I3C and a cocktail of protease inhibitors were from Sigma (St Louis, MO). NNK was synthesized as described [18]. All primary antibodies used for Western immunoblotting studies were purchased from Cell Signaling Technology (Beverly, MA). Multiplex protein arrays and the reagents required for protein array studies were obtained from R and D (Minneapolis, MN). All the reagents for Ki-67 immunohistochemistry studies were obtained from Dako (Carpinteria, CA). Mouse diets (AIN-93G and AIN-93M) were purchased from Harlan Teklad (Madison, WI). The AIN-93G diet, high in protein and fat, was used to support rapid growth of the mice during early age, whereas AIN-93M diet, low in protein and fat, was used for maintenance and growth.

2.2. Tumor bioassay

Female A/J mice, 5–6 weeks of age, were obtained from The Jackson Laboratory (Bar Harbor, ME). Upon arrival (Week 0), the mice were housed in the specific pathogen-free animal quarters of Research Animal Resources (RAR), University of Minnesota Academic Health Center, and randomized into six groups. One week after arrival, mice in groups 1–4 received four intraperitoneal injections of NNK (50 mg/kg, in 0.1 ml physiological saline solution, twice a week for two consecutive weeks). Mice in group 5 and 6 were used as negative controls and received 0.1 ml of physiological saline solution. Subsequently, mice in group 3 and 4 were given I3C in the diet (10 μmol/g diet) during the post initiation phase (week 4–27) or during the tumor progression phase (week 28–52), respectively. In previous studies, I3C at a dose level of 10 μmol/g diet showed a significant effect against lung tumorigenesis without causing toxic effects [17). Mice in groups 1, 2, 5, and 6 were maintained on non-supplemented AIN-93 diet. The treatment protocols are depicted in Figure 1A. Food consumption levels and body weights were monitored weekly and bi-weekly, respectively, during the whole period of the study. The experiments were terminated

either at week 27 (groups 1, 3, and 5) or at week 52 (groups 2, 4, and 6) using an overdose of carbon dioxide. Subsequently, the lungs were harvested, the number and size of lung tumors on the surface of the lung were determined under a dissecting microscope. All left lung lobes from carcinogen-treated mice and controls were preserved in 10% buffered formalin for subsequent histopathological and Ki-67 expression analyses. Tumors on the remaining lung lobes of carcinogen-treated mice were microdissected and stored, together with the right lung lobes from control mice, at −80°C for subsequent Western immunoblotting studies.

2.3. Histopathological analysis

Randomly selected, formalin-fixed lung tissues were processed through a series of graded alcohols, embedded in paraffin and three step sections (each 200 μm apart) having a thickness of 4 μm were cut and stained with hematoxylin and eosin. Proliferative lesions were counted in each step section and the total number of each type of lesion per mouse was expressed as an average number of each lesion per section (sum of each lesion in three step sections divided by three).

Proliferative lesions in the lungs were classified as hyperplasia, adenoma, adenoma with dysplasia or adenocarcinoma based on our previous reports (Kassie et al., 2010; Dagne et al., 2011) and the recommendations published by the Mouse Models of Human Cancers Consortium [19]. The category adenoma with dysplasia (also known as adenoma with cellular pleomorphism or adenoma with progression) is an adenoma in which ≥10 cells are pleomorphic, characterized by large cell and/or nuclear size; increased cytoplasmic-to-nuclear ratio; prominent nucleoli; nuclear crowding and increased numbers of mitotic figures with no evidence of parenchymal invasion by pleomorphic cells [16,17].

2.4. Ki-67 analysis of lung tissues

Assessment of Ki-67 positive cells was carried out as described previously (Dagne et al., 2008). Briefly, 4-μm formalin-fixed paraffin sections from lung tissues of mice sacrificed at week 27 were deparaffinized and antigen retrieved by incubating the slides in a pressure cooker in citrate buffer (pH 6.0) for 30 s at 121°C and 10 s at 90°C followed by cooling for 15 min. Endogenous peroxidase was blocked with 3% hydrogen peroxide for 15 min at room temperature. The sections were incubated with a universal protein block for 10 min, followed by a 60-min room temperature incubation with rat monoclonal antibody against mouse Ki-67 diluted at 1:50. Sections were then incubated for 30 min at room temperature with biotinylated antirat secondary antibody (Vector) diluted at 1:300. Binding was detected by incubating sections with streptavidin/horseradish peroxidase for 20 min at room temperature followed by diaminobenzidine chromagen application for 5 min at room temperature. Sections were counterstained with Mayer's hematoxylin. For negative control slides, the primary antibody was substituted by Super Sensitive Negative Control Rat serum (Biogenix). Photomicrograph images for Ki-67 were captured with an attached camera linked to a computer. The Ki-67 labeling index was calculated as the percentage of Ki-67-positive tumor cells that showed brown nuclear staining among 1,700 tumor cells, counted in seven fields, for each of a total of 48 lesions (8 lesions each for hyperplastic foci, adenoma and adenoma with dysplasia from different mice) from NNK or NNK plus I3C groups

2.5. Proteome profiler array

We used human phospho-receptor tyrosine kinase, human phospho-kinase and human apoptosis antibody arrays from R and D (Minneapolis, MN) to assess the effect of I3C on cancer related kinome and pro-apoptotic and anti-apoptotic proteins at a global level. The experiments were carried out according to the manufacturer`s recommendations. Briefly, 1×

10^7 A549 cells were treated with I3C at a concentration of 300 μM, which is the IC_{50} of the compound in these cells after treatment for 72 h [17]. Subsequently, the cells were lysed in 1 ml of lysis buffer and the protein concentrations determined using a BCA protein assay kit (Pierce, Rockford, IL). Diluted cell lysates containing 500-μg protein were prepared and added to nitrocellulose membrane containing capture and control antibodies in duplicate. After incubation at 4°C overnight, the membrane was washed three times and incubated with reconstituted detection antibody at room temperature for 2 h. Subsequently, membrane was washed three times, incubated with diluted streptavidin-HRP for 30 min at room temperature, washed again and signals detected using the chemiluminescent detection reagent (Pierce, Rockford, IL). The films were scanned and analyzed using the image analysis software UN-SCAN-IT (Silk Scientific, Orem, UT). On the basis of comparative protein expression changes in proteome profiler array and Western immunoblotting, expression changes by 30% or more, compared to the level in DMSO-treated A549 cells, were considered significant.

2.6. Western immunoblot analyses

To prepare protein lysates from A549 cells, about 1×10^6 cells were treated with dimethyl sulfoxide or I3C (300 μM) for 72 h, harvested and suspended for 1 h in a lysis buffer composed of the following constituents: Fifty mmol/L Tris-HCl, 150 mmol/L NaCl, 1 mmol/L EGTA, 1 mmol/L EDTA, 20 mmol/L, 1% Triton X-100, pH 7.4, and protease inhibitors [aprotinin (1 μg/mL), leupeptin (1 μg/mL), pepstatin (1 μmol/L), and phenylmethylsulfonyl fluoride (0.1 mmol/L)] and phosphatase inhibitors Na_3VO_4 (1 mmol/L) and NaF (1 mmol/L).The preparations were centrifuged (14,000 × g for 20 min) and supernatants stored at −80°C.

Protein samples from mouse lung tissues were prepared as follows. About 30 mg of normal lung tissue (from vehicle-treated control mice) or microdissected tumors (from NNK-treated or NNK plus I3C-treated mice) were pooled from six mice per group, ground using a mortar and pestle and the resulting lung tissue powder was homogenized in an ice-cold lysis buffer containing similar components as used for A549 cells. Subsequently, the homogenates were centrifuged (14,000 × g for 25 min at 4°C) and the supernatants collected, aliquoted and stored at −80°C..

For Western immunoblotting, 60 μg of protein were loaded onto a 4% to 12% Novex Tris-glycine gel (Invitrogen) and run for 60 min at 200 V. The proteins were then transferred onto a nitrocellulose membrane (Bio-Rad) for 1 h at 30 V. Protein transfer was confirmed by staining membranes with BLOT-FastStain (Chemicon). Subsequently, membranes were blocked in 5% Blotto nonfat dry12 milk in Tris buffer containing 1% Tween 20 for 1 h and probed overnight with the following primary antibodies obtained from Cell Signaling Technology (Beverly, MA): anti-phospho-Akt, anti-Akt, anti-phospho-ERK, anti-ERK, anti-survivin, anti-phospho-β-catenin, anti-phospho-mTOR, anti-phospho-STAT3, anti-phopsho-FAK, anti-phopsho-p53, anti-chk2, anti-phospho-CREB, anti-phospho-JNK, anti-phospho-p38, anti-phospho-EGFR, anti-phospho c-Met, anti-phospho-erbB2, anti-phospho-erbB3, anti-phospho-IGFR1, anti-PARP and anti-beta-actin. All primary antibodies were used at a dilution of 1:1,000. After incubating the membranes with a secondary antibody (goat anti-rabbit IgG; 1:5,000) for 1 h, chemiluminescent immunodetection was used. Signal was visualized by exposing membranes to HyBolt CL autoradiography film. All membranes were stripped and reprobed with anti-β-actin (1:1000) to check for differences in the amount of protein loaded in each lane. For each protein, at least three Western assays were carried out. Densitometric measurements of the bands were done with digitalized scientific software program UN-SCAN-IT purchased from Silk Scientific Corporation (Orem, UT).

2.7. Statistical analysis

Wilcoxon rank sum test was used for pair-wise comparisons of the number and size of tumors on the surface of the lung (groups treated with NNK and received I3C versus the group treated with NNK only). Since the outcome variables were approximately normally distributed, two-sample-t-test was employed for the pair-wise comparison of the frequency of the different histopathological lesions (hyperplasia, adenoma, adenoma with dysplasia and adenocarcinoma) between groups treated with NNK and given I3C versus the groups treated with NNK only. Two-sided *p*-values ≤ 0.05 were considered statistically significant. All analyses were conducted in SAS 9.1.3. For the analyses of results from the Ki-67 labeling index assay, the two-sided Student's *t* test was used. *P* values of ≤ 0.05 were considered statistically significant. Statistical analysis of continuous data (body weight and food consumption) was performed using analysis of variance, with post hoc comparisons made using Dunnett's test.

3. Results

3.1. Effects of I3C on the multiplicity of NNK-induced lung tumors

Supplementation of the mouse diet with I3C did not have a significant effect on food consumption or body weight of the animals. The final body weight of mice treated with NNK and given I3C was reduced by 3% and 4% at week 27 and week 52, respectively (Fig. 1B), compared to mice treated with NNK alone. Food consumption levels were slightly increased in mice maintained on I3C-supplemented diet as compared to mice given the basal diet (data not shown).

Multiplicities of lung tumors in mice treated with NNK alone or NNK plus I3C are shown in Table 1. Mice treated with NNK and terminated at week 27 had 39.9 ± 9.0 tumors/mouse. Upon supplementation of the diet with I3C during week 4–27 (post-initiation protocol), tumor multiplicities were significantly reduced to 19.4 ± 4.8/mouse, corresponding to a significant reduction by 49%. On the other hand, administration of I3C to NNK-treated mice during week 28–52 (progression protocol) did not reduce the number of tumors. Lung tumor multiplicities of mice treated with NNK plus I3C and NNK alone were 45.4 ± 5.9 tumors/mouse and 44.7 ± 6.1 tumors/mouse, respectively.

We also determined the size of the tumors on the surface of the lung and categorized the tumor sizes into four groups: < 0.5 mm, 0.5 – 1 mm, > 1 mm but < 2 mm and ≥ 2 mm for tumors harvested at week 27 and < 1 mm, 1 – 2 mm, > 2 mm but < 3 mm and ≥ 3 mm for tumors harvested at week 52. In mice given I3C and terminated at week 27, multiplicities of tumors with a size of < 0.5 mm, 0.5 – 1 mm, > 1 mm but < 2 mm and ≥ 2 mm were reduced by 25% ($p < 0.084$), 43% ($p < 0.0382$), 66% ($p < 0.0017$), and 83% ($p < 0.0001$) as compared to the NNK group given basal diet (Fig. 2A, left panel). In mice given I3C and terminated at week 52, multiplicities of tumors with a size of < 1mm and 1–2 mm were increased by 295% ($p < 0.0001$) and 133% ($p < 0.001$), respectively, as compared to the NNK group given the basal diet, whereas tumors with a size of > 2 mm but < 3 mm and ≥ 3 mm were reduced by 56% ($p < 0.0024$) and 57% ($p < 0.0021$), respectively (Fig. 2 right panel).

3.2. Effects of I3C on NNK-induced histopathological lesions

To determine the effect of I3C on NNK-induced pulmonary microscopic lesions, lung tissues were analyzed histopathologically and the lesions classified, based on established criteria [19], as hyperplastic foci, adenoma, adenoma with dysplasia, and adenocarcinoma. In mice treated with NNK alone and terminated at week 27, multiplicities of hyperplastic foci, adenoma, adenoma with dysplasia, and adenocarcinoma were 4.6 ± 0.4, 6.2 ± 0.8, 2.4 ±

0.8, and 0.7 ± 0.1, respectively. Dietary administration of I3C decreased multiplicities of hyperplastic foci, adenoma, adenoma with dysplasia, and adenocarcinoma to 2.2 ± 0.2 ($p < 0.0021$), 3.1 ± 0.3 ($p < 0.0019$), 0.6 ± 0.1 ($p < 0.0001$) and 0.1 ± 0.04 ($p < 0.0001$), corresponding to a 52%, 50%, 75% and 85% reduction, respectively (Fig. 2B, left panel). In mice treated with NNK plus I3C and terminated at week 52, multiplicities of hyperplastic foci and adenoma were significantly increased by 67% and 58%, respectively, as compared to the NNK group (3.9 ± 0.3 hyperplastic foci/mouse in the NNK plus I3C group versus 1.3 ± 0.4 lesions/mouse in the NNK group, $p < 0.0016$; 7.4 ± 0.3 adenoma lesions/mouse in the NNK plus I3C group versus 3.1 ± 0.6 lesions/mouse in the NNK group, $p < 0.0041$). However, I3C treatment significantly decreased multiplicities of adenoma with dysplasia and adenocarcinoma by 78% and 93%, respectively (1.1 ± 0.1 adenoma with dysplasia lesions/mouse in the NNK plus I3C group versus 4.9 ± 0.8 lesions/mouse in the NNK group, $p < 0.0001$; 0.14 ± 0.04 adenocarcinoma lesions/mouse in the NNK plus I3C group versus 2.1 ± 0.3 lesions/mouse in the NNK group, $p < 0.0001$, Fig. 2B, right panel).

3.3. I3C reduced the expression of cell proliferation- and survival- related proteins in lung tumors

To shed some light on the potential mechanisms through which I3C inhibited NNK-induced lung adenocarcinoma, we compared levels of Ki-67-labelling index and phospho-Akt, phospho-ERK, survivin and cleaved PARP in the NNK group versus NNK plus I3C group. Representative photomicrographs showing Ki-67-labeling index (as indicated by dark-brown spots in the nuclei) in lung adenoma from NNK- or NNK plus I3C-treated mice and normal lung tissues from vehicle-treated mice are shown in Fig 2C. In mice treated with NNK alone, the percentages of Ki-67-positive lung cells in hyperplastic foci, adenoma and adenoma with dysplasia lesions were 2.2 ± 03, 2.4 ± 0.4, and 1.9 ± 0.2, respectively. In the NNK plus I3C-treated group the percentages of Ki-67-positive cells in hyperplastic foci, adenoma and adenoma with dysplasia were 0.4 ± 0.1, 0.8 ± 0.2 and 0.6 ± 0.3, respectively, corresponding to a significant reduction by 82%, 86% and 68%.

Similarly, Western blotting studies showed a higher expression of phospho-Akt and survivin in NNK-induced lung tumors compared to the level in normal lung tissues from vehicle-treated mice (Fig. 2D). In lung tissues from mice treated with NNK plus I3C, the levels of phospho-Akt and survivin were markedly reduced as compared to the expression of these proteins in the NNK group. In line with these results, apoptosis of tumor cells, as evidenced by PARP-cleavage, was enhanced in lung tissues of mice given I3C-supplemented diet. Unexpectedly, expression of phospho-ERK was increased by I3C, compared to the level in mice treated with control diet.

3.4. Modulation by I3C of phospho-kinases and apoptosis-related proteins in A549 cells

In order to identify the full spectrum of proteins that are targeted by I3C, we compared, using proteome profiler array, activation status of several receptor tyrosine kinases and intracellular serine/threonine/tyrosine kinases and expression of apoptosis-related proteins in I3C-treated and untreated A549 cells. Activation of 10 receptor tyrosine kinases was modulated in response I3C treatment (p-EGFR, p-ErbB2, p-ErbB3, p-c-Met, p-Flt3, p-FGFR, p-VEGF, p-IGFR-1, PDGF, and p-m-CSFR). Of these, activation of nine proteins was reduced, the effect on p-ErbB3, p-c-Met and p-VEGF-R3 being the strongest (66–70%), whereas, quite unexpectedly, p-EGFR increased (Fig. 3A). Among intracellular serine/threonine/tyrosine kinases, activation of 11 phospho-proteins was modulated by I3C. p-53, p-chk2, p-p38, p-JNK and p-ERK increased, whereas p-CREB, p-mTOR, p-Src, p-Hck, p-FAK, p-STAT3, p-beta-catenin and p-Akt decreased; the reduction in p-Akt, p-beta-catenin and p-FAK was the highest, Fig. 3B. Similarly, I3C modulated levels of 10 apoptosis-related proteins (Fig. 3C).The expression of pro-apoptotic proteins Bax, TRAIL, Fas, and cleaved

caspase 3 increased, whereas levels of the anti-apoptotic proteins Bcl-2, HIF-1α, IAP, survivin and claspin were decreased. To verify these results, selected phospho-kinases were analyzed by Western immunoblotting. With the exception of p-EGFR, which was increased in the studies with protein arrays but decreased in immunoblot assays, the results were similar to those found in protein arrays (Fig. 3D). However, the changes observed in immunoblot studies were stronger.

4. Discussion

In the present study, we examined inhibition by I3C of NNK-induced lung adenocarcinoma in mice given the chemopreventive agent either during the post-initiation phase or tumor progression phase. In the post-initiation protocol, chemopreventive agents are given 2–3 weeks post-carcinogen initiation and continued until tumors are formed, whereas the tumor progression protocol is designed to determine effects on tumor progression to carcinoma by administering preventive agents beginning around the time tumors are formed. Testing the efficacy of chemopreventive agents during the tumor progression phase is more relevant than the post-initiation protocol since this phase of lung tumorigenesis is frequently targeted in human clinical chemoprevention trials. Although our earlier studies showed that I3C administered to mice during the post-initiation phase inhibited vinyl carbamate-induced [16] or NNK-induced [17] lung adenocarcinoma, to our knowledge, this is the first report on the efficacy of I3C to delay malignant tumor progression to adenocarcinoma when given in the progression protocol. Moreover, we assessed, for the first time, modulation by I3C of cancer-related kinome and pro-apoptotic and anti-apoptotic proteins in A549 cells on a global level.

Administration of I3C during week 4–27 (post-initiation protocol) reduced the multiplicity all tumor size classes, albeit at different efficacy levels, and all forms of histological lesions (hyperplastic foci, adenoma, adenoma with dysplasia, and adenocarcinoma). On the other hand, when I3C was given during week 28–52 (tumor progression phase), multiplicities of smaller tumors (≤ 2 mm) increased, whereas that of bigger tumors (> 2 mm) decreased. Similarly, multiplicities of early stage histological lesions increased, whereas advanced lesions (adenoma with dysplasia and adenocarcinoma) decreased. Despite these differences, I3C effectively inhibited the development of pulmonary adenocarcinoma when administered during the progression phase, the most critical stage in lung cancer development.

In an attempt to identify potential mechanisms for the lung cancer preventive activities of I3C, we examined modulation by the compound of cell proliferation- and apoptosis-related proteins in lung tissues and receptor tyrosine kinases, non-receptor kinases and pro-and anti-apoptotic proteins in A549 cells. Since Akt is frequently activated during lung tumorigenesis [20–22] and our earlier reports showed that Akt was activated in carcinogen-induced mouse lung tumors and I3C suppressed its activation [16,17], our focus was on Akt and related proteins. AKT, a major downstream target of growth factor receptor tyrosine kinases that signals via phosphatidylinositol-3 kinase (PI3K), plays a central role in tumor cell survival, growth, migration, and angiogenesis [23]. Immunoblotting studies in mouse lung tissues showed that I3C reduced expression of phospho-Akt and its downstream target, survivin, but enhanced PARP cleavage, a marker for apoptosis. In subsequent studies using A549 cells, we showed that I3C inhibited activation of receptor tyrosine kinases such as ErbB2, ErbB3, c-Met, VEGF receptors and IGFR-1, all of which are known to be over-expressed in human lung cancer and enhance activation of Akt via a phosphatidyliositoal-3 kinase (PI3K)-dependent pathway [24–27]. Although our results on inactivation of EGFR by I3C were inconsistent, EGF-induced over-activation of Akt was inhibited by I3C (data not shown), which indicated that I3C blocks the EGFR/PI3K/Akt signaling pathway. In a previous

report, I3C abrogated EGFR expression and activation and EGF-induced activation of PI3K and Akt in prostate cancer cells [28].

Intracellular serine/threonine/tyrosine kinases that were modulated by I3C include Akt itself, Src, Hck, FAK, STAT3, CREB, mTOR, beta-catenin, p53, Ch2, and the MAPKs ERK, p38 and JNK. Src and Hck are members of the Src family of non-receptor tyrosine kinases and increased expression of Src has been reported in 60%–80% of lung adenocarcinomas and bronchioloalveolar cancers and in 50% of squamous cell carcinomas [29]. The main pathways through which Src increases tumor cell survival is via its down-stream effectors, STAT3, and FAK, both of which are transcription factors that mediate expression of genes involved in cell cycle progression and apoptosis. STAT3 and FAK are down-stream effectors of the PI3K/Akt pathway [30,31]. Similarly, CREB, a transcription factor down-stream of the PI3K/Akt pathway, activates the expression of genes related to cell survival, inflammation and proliferation such as Bcl-2, Bcl-xl, cyclooxygenase-2, and tumor necrosis factor-α [32]. The most widely studied down-stream effector of Akt is mTOR, which has been shown to be over-expressed in 74% of NSCLC [33]. Although some mTOR inhibitors such as rapamycin are known to induce upstream receptor tyrosine kinase signaling and thereby activate Akt in both cancer cells and in patient tumors [34], I3C inhibited activation of both proteins. Another protein whose function is intimately associated with Akt is p53. Akt and p53 are major but opposing players in signaling pathways that regulate cell survival. p53 counteracts the effects of Akt via promotion of caspase-mediated cleavage and subsequent degradation of the AKT protein itself and induction of PTEN expression [35]. However, comparison the apoptotic effects of I3C in p53 wild type and p53 mutant lung cancer cells and in A549 cells pretreated with pifithrin-α, a small molecule inhibitor of p53, did not show any differences (data not shown), indicating that p53 is probably not necessary for the chemopreventive effects of I3C in these cells.

Activation of the MAPK proteins JNK and p38 by I3C indicates involvement of cellular stress responses in the antiproliferative and apoptotic effects of the compound in A549 cells. However, activation by I3C of ERK in both A549 cells and mouse lung tissues is intriguing since this protein is often associated with mitogenic effects. Indeed, similar effects were observed in prostate cancer cells treated with I3C or phenethyl isothiocyanate [36,37] and colon cancer cells treated with selenomethionine [38]. Phenethyl isothiocyanate-induced apoptosis in prostate cancer cells was even dependent on ERK activation since pharmacological inhibition of ERK activation abolished the apoptotic effect of the chemopreventive agent [37]. Activation of ERK was also shown to inhibit CDK activity and induce cell cycle arrest and these effects were blocked by the pharmacological inhibitor of ERK [39]. All these studies indicate that ERK activation, in addition to its well-known mitogenic effects, could also be a negative effector of cell growth and survival. The differential effect of ERK on cell proliferation and survival was found to be correlated with the intensity and duration of ERK activation, i.e., persistent activation of ERK leads to cell cycle arrest, whereas transient activation of the protein increases cell proliferation [36].

Studies in mice and human volunteers showed that I3C was metabolized quickly and completely into more than 18 products [9]. The parent compound was not detected in the plasma or tissues 1 h after administration [40,41]. On the other hand, under cell culture conditions, only 0.3% of I3C enters the cells and the compound was surprisingly inert to metabolism with a half-life in medium of approximately 40 h [42]. In this study, only a fraction of the intracellular I3C was converted into diindolylmethane. Thus, the high concentration of I3C required in the present studies could be related to the poor intracellular accumulation and metabolism of I3C in cell culture models. I3C was also found to be stable when left in the open in the mouse feeders [43].

In conclusion, our results showed that I3C is a potent inhibitor of lung adenocarcinoma in mice when given during the early phase of lung tumorigenesis or after tumors had developed, indicating the potential of the compound not only to prevent lung cancer but for therapy as well. The major mechanism through which I3C inhibited lung adenocarinoma is modulation of activation of proteins in the RTK/PI3K/Akt/ pathway. The exact role of each protein in the pathway remains to be determined.

Acknowledgments

This study was funded by a research grant from NIH to FK (CA-128801). We thank Bob Carlson for help in the preparation of the Figures and Melissa Schutten, Josh Parker and Paula Overn, from Comparative Pathology Shared Resource, for help with the mouse necropsy, tumor count and histopathological and immunohistochemical analysis of mouse lung tissues.

References

1. Lam TK, Ruczinski I, Helzlsouer KJ, Shugart YY, Caulfield LE, Alberg AJ. Cruciferous vegetable intake and lung cancer risk: a nested case-control study matched on cigarette smoking. Cancer Epidemiol. Biomarkers Prev. 2010; 19 2534-1540.
2. Boggs DA, Palmer JR, Wise LA, Spiegelman D, Stampfer MJ, Adams-Campbell LL, Rosenberg L. Fruit and vegetable intake in relation to risk of breast cancer in the Black Women's Health Study. Am. J. Epidemiol. 2010; 172:1268–1279. [PubMed: 20937636]
3. Tang L, Zirpoli GR, Guru K, Moysich KB, Zhang Y, Ambrosone CB, McCann SE. Intake of cruciferous vegetables modifies bladder cancer survival. Cancer Epidemiol. Biomarkers Prev. 2010; 19:1806–1811. [PubMed: 20551305]
4. Dolecek TA, McCarthy BJ, Joslin CE, Peterson CE, Kim S, Freels SA, Davis FG. Prediagnosis food patterns are associated with length of survival from epithelial ovarian cancer. J. Am. Diet Assoc. 2010; 110:369–382. [PubMed: 20184987]
5. Tookey, HL.; VanEtten, CH.; Daxenbichler, ME. Glucosinolates. In: Liener, IE., editor. Toxic constituents of plant stuffs. New York: Academic Press; 1980. p. 103-142.
6. McDanell R, McLean AEM, Hanley AB, Heaney RK, Fenwick GR. Chemical and biological properties of indole glucosinolates (glucobrassicins): a review. Food Chem. Toxicol. 1988; 26:59–70. [PubMed: 3278958]
7. Fahey JW, Zalcmann AT, Talalay P. The chemical diversity and distribution of glucosinolates and isothiocyanates among plants. Phytochemistry. 2001; 56:5–51. [PubMed: 11198818]
8. Hecht SS, Carmella SG, Kenney PM, Low SH, Arakawa K, Yu MC. Effects of cruciferous vegetable consumption on urinary metabolites of the tobacco-specific lung carcinogen 4-(methylnitrosamino)-1-(3-pyridyl)-1-butanone in singapore chinese. Cancer Epidemiol. Biomarkers Prev. 2004; 13:997–1004. [PubMed: 15184256]
9. Aggarwal BB, Ichikawa H. Molecular targets and anticancer potential of indole-3-carbinol and its derivatives. Cell Cycle. 2005; 4:1201–1215. [PubMed: 16082211]
10. Kim EJ, Park H, Kim J, Park JH. 3,3'-diindolylmethane suppresses 12-O-tetradecanoylphorbol-13-acetate-induced inflammation and tumor promotion in mouse skin via the downregulation of inflammatory mediators. Mol. Carcinog. 2010; 49:672–683. [PubMed: 20564344]
11. Rahman KW, Li Y, Wang Z, Sarkar SH, Sarkar FH. Gene expression profiling revealed survivin as a target of 3,3'-diindolylmethane-induced cell growth inhibition and apoptosis in breast cancer cells. Cancer Res. 2006; 66:4952–4960. [PubMed: 16651453]
12. Kong D, Li Y, Wang Z, Banerjee S, Sarkar FH. Inhibition of angiogenesis and invasion by 3,3'-diindolylmethane is mediated by the nuclear factor-kappaB downstream target genes MMP-9 and uPA that regulated bioavailability of vascular endothelial growth factor in prostate cancer. Cancer Res. 2008; 67:3310–3319. [PubMed: 17409440]
13. Kong D, Banerjee S, Huang W, Li Y, Wang Z, Kim HR, Sarkar FH. Mammalian target of rapamycin repression by 3,3'-diindolylmethane inhibits invasion and angiogenesis in platelet-derived growth factor-D-overexpressing PC3 cells. Cancer Res. 2008; 68:1927–1934. [PubMed: 18339874]

14. IARC. Cruciferous vegetables, isothiocyanates and indoles. Vol. Vol. 9. Lyon: IARC Printing Press; 2004. IARC handbooks of cancer prevention; p. 171-176.
15. Minich DM, Bland JS. A review of the clinical efficacy and safety of cruciferous vegetable phytochemicals. Nutr. Rev. 2007; 65:259–267. [PubMed: 17605302]
16. Kassie F, Kalscheuer S, Matise I, Ma L, Melkamu T, Upadhyaya P, Hecht SS. Inhibition of vinyl carbamate-induced pulmonary adenocarcinoma by indole-3-carbinol and myo-inositol in A/J mice. Carcinogenesis. 2010; 31:239–245. [PubMed: 19625346]
17. Dagne A, Melkamu T, Schutten MM, Qian X, Upadhyaya P, Luo X, Kassie F. Enhanced inhibition of lung adenocarcinoma by combinatorial treatment with indole-3-carbinol and silibinin in A/J mice. Carcinogenesis. 2011; 32:561–567. [PubMed: 21273642]
18. Hecht SS, Lin D, Castonguay A. Effects of α-deuterium substitution on the mutagenicity of 4-(methylnitrosamino)-1-(3-pyridyl)-1-butanone (NNK). Carcinogenesis. 1983; 4:305–310. [PubMed: 6339096]
19. Nikitin AY, Alcaraz A, Anver MR, Bronson RT, Cardiff RD, Dixon D, et al. Classification of proliferative pulmonary lesions of the mouse: recommendations of the mouse models of human cancers consortium. Cancer Res. 2004; 64:2307–2316. [PubMed: 15059877]
20. Tsao AS, McDonnell T, Lam S, Putnam JB, Bekele N, Hong WK, Kurie JM. Increased phospho-AKT (Ser(473)) expression in bronchial dysplasia: implications for lung cancer prevention studies. Cancer Epidemiol. Biomarkers Prev. 2003; 12:660–664. [PubMed: 12869408]
21. Massion PP, Taflan PM, Shyr Y, Rahman SM, Yildiz P, Shakthour B, Edgerton ME, Ninan M, Andersen JJ, Gonzalez AL. Early involvement of the phosphatidylinositol 3-kinase/Akt pathway in lung cancer progression. Am. J. Respir. Crit. Care Med. 2004; 170:1088–1094. [PubMed: 15317667]
22. Balsara BR, Pei J, Mitsuuchi Y, Page R, Klein-Szanto A, Wang H, Unger M, Testa JR. Frequent activation of AKT in non-small cell lung carcinomas and preneoplastic bronchial lesions. Carcinogenesis. 2004; 25:2053–2059. [PubMed: 15240509]
23. Liao Y, Hung MC. Physiological regulation of Akt activity and stability. Am. J. Transl. Res. 2010; 2:19–42. [PubMed: 20182580]
24. Yarden Y, Sliwkowski MX. Untangling the ErbB signaling network. Nat. Rev. Mol. Cell Biol. 2001; 2:127–137. [PubMed: 11252954]
25. Olivero M, Rizzo M, Madeddu R, Casadio C, Pennacchietti S, Nicotra MR, Prat M, Maggi G, Arena N, Natali PG, Comoglio PM, Di Renzo MF. Overexpression and activation of hepatocyte growth factor/scatter factor in human non-small-cell lung carcinomas. Br. J. Cancer. 1996; 74:1862–1868. [PubMed: 8980383]
26. Han H, Silverman JF, Santucci TS, et al. Vascular endothelial growth factor expression in stage I non-small cell lung cancer correlates with neoangiogenesis and a poor prognosis. Ann. Surg. Oncol. 2001; 8:72–79. [PubMed: 11206229]
27. Dziadziuszko R, Camidge DR, Hirsch FR. The insulin-like growth factor pathway in lung cancer. J. Thoracic Oncol. 2008; 3:815–818.
28. Chinni SR, Sarka FH. Akt inactivation is a key event in indole-3-carbinol-induced apoptosis in PC-3 cells. Clin Cancer Res. 2002; 8:1228–1236. [PubMed: 11948137]
29. Mazurenko NN, Kogan EA, Zborovskaya IB, et al. Expression of pp60c-src in human small cell and non-small cell lung carcinomas. Eur. J. Cancer. 1992; 28:372–377. [PubMed: 1375484]
30. Turečcková J, Vojtěchová M, Krausová M, Šloncová E, Kořínek V. Focal adehesion kinase functions as an Akt downstream target in migration of colorectal cancer cells. Trans.Oncol. 2009; 2:281–290.
31. Han S, Yun H, Son D, Tompkins VS, Peng L, Chung S, Kim J, Park E, Janz S. NF-κB/STAT3/PI3K signaling crosstalk in iMyc$^{E\mu}$ B lymphoma. Molecular Cancer. 2010; 9:97. [PubMed: 20433747]
32. Aggarwal S, Kim S, Ryu S, Chung W, Koo JS. Growth suppression of lung cancer cells by targeting cyclic AMP response element-binding protein. Cancer Res. 2008; 68:981–986. [PubMed: 18281471]

33. Balsara BR, Pei J, Mitsuuchi Y, Page R, Klein-Szanto A, Wang H, Unger M, Testa JR. Frequent activation of AKT in non-small cell lung carcinomas and preneoplastic bronchial lesions. Carcinogenesis. 2004; 25:2053–2059. [PubMed: 15240509]
34. O'Reilly KE, Rojo F, She Q, Solit D, Mills GB, Smith D, Lane H, Hofmann F, Hicklin DJ, Ludwig DL, Baselga J, Rosen N. mTOR inhibition induces upstream receptor tyrosine kinase signaling and activates Akt. Cancer Res. 2006; 66:1500–1508. [PubMed: 16452206]
35. Haupt S, Berger M, Goldberg Z, Haupt Y. Apoptosis - the p53 network. J. Cell Science. 2003; 116:4077–4085. [PubMed: 12972501]
36. Wang Z, Zhang B, Wang M, Carr BI. Persistent ERK phosphorylation negatively regulates cAMP response element-binding (CREB) activity via recruitment of CREB-binding protein to pp90. J.Biol. Chem. 2003; 278:11138–11144. [PubMed: 12540838]
37. Xiao D, Singh SV. Phenethyl isothiocyanate-induced apoptosis in p53-deficient PC-3 human prostate cancer cell line is mediated by extracellular signal-regulated kinases. Cancer Research. 2002; 62:3615–3619. [PubMed: 12097262]
38. Goulet A, Chigbrow M, Frisk P, Nelson MA. Selenomethionine induces sustained ERK phosphorylation leading to cell-cycle arrest in human colon cancer cells. Carcinogenesis. 2005; 126:109–117. [PubMed: 15513932]
39. Pumiglia KM, Decker SJ. Cell cycle arrest mediated by the MEK/mitogen-activated protein kinase pathway. Proc Natl Acad Sci U S A. 1997; 94:448–452. [PubMed: 9012803]
40. Anderton MJ, Manson MM, Verschoyle RD, Gescher A, Lamb JH, Farmer PB, Steward WP, Williams ML. Pharmacokinetics and tissue disposition of indole-3-carbinol and its acid condensation products after oral administration to mice. Clin Cancer Res. 2004; 10:5233–5241. [PubMed: 15297427]
41. Reed GA, Arneson DW, Putnam WC, Smith HJ, Gray JC, Sullivan DK, Mayo MS, Crowell JA, Hurwitz A. Single-dose and multiple-dose administration of indole-3-carbinol to women: pharmacokinetics based on 3,3'-diindolylmethane. Cancer Epidemiol Biomarkers Prev. 2006; 15:2477–2481. [PubMed: 17164373]
42. Staub RE, Feng C, Onisko B, Bailey GS, Firestone GL, Bjeldanes LF. Fate of indole-3-carbinol in cultured human breast tumor cells. Chem Res Toxicol. 2002; 15:101–109. [PubMed: 11849035]
43. Kassie F, Matise I, Negia M, Upadhyaya P, Hecht SS. Dose-dependent inhibition of tobacco smoke carcinogen-induced lung tumorigenesis in A/J mice by indole-3-carbinol. Cancer Prev Res. 2008; 1:568–576.

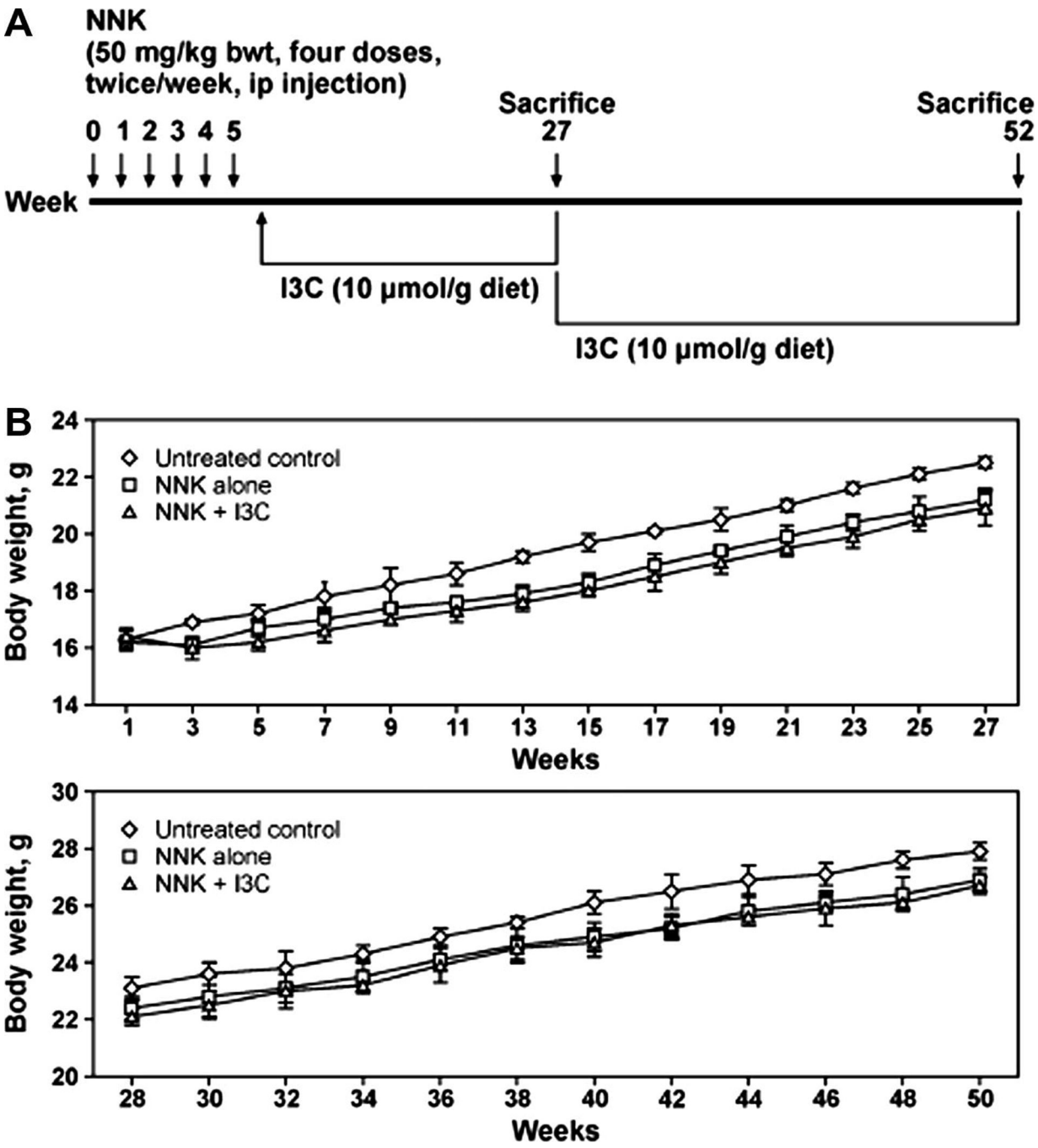

Figure 1.

Mean body weight curves of mice given I3C in the diet. I3C was administered to mice following the protocol depicted (A) and the body weights measured biweekly either from week 1–27 (B, upper panel for post-initiation protocol) or week 28–50 (B, lower panel for progression protocol).

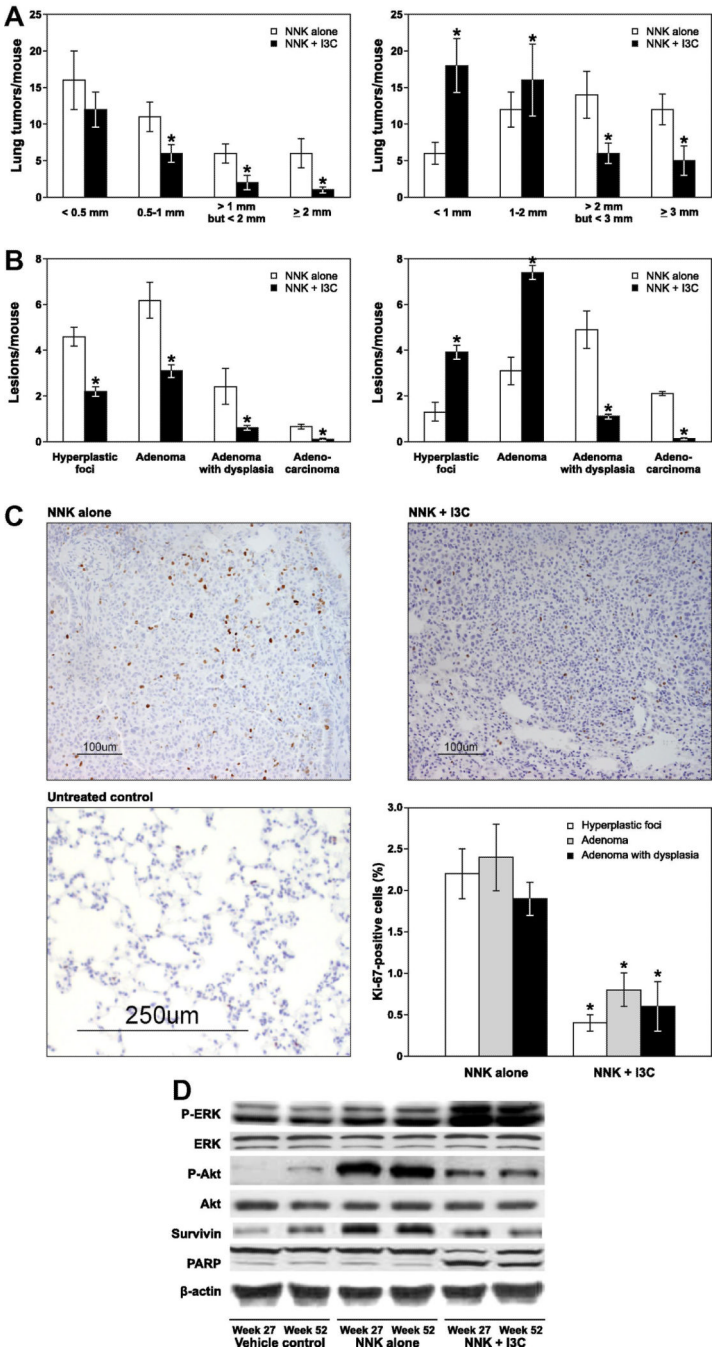

Figure 2.

Effects I3C on NNK-induced lung tumorigenesis. A, Multiplicities of tumors on the surface of the lung. The size of surface tumors on lungs of mice was estimated using the calibrated scale in the eyepiece of a dissecting microscope. Each tumor was assigned to one of the following categories: < 0.5, 0.5 – 1, > 1 but < 2, and > 2 mm for 27 week study (left panel) and < 1, 1 – 2, > 2 but < 3, and > 3 mm for week 52 study (right panel); *, $P < 0.05$. B, multiplicities of histopathological lesions. Frequencies of pulmonary hyperplastic foci, adenoma, adenoma with dysplasia and adenocarcinoma were determined as described in the Materials and Methods in tissue samples collected at week 27 (left panel) and week 52 (right panel). C, Photomicrographs (×20) of Ki-67–stained lung tissues from mice treated with

NNK alone, NNK plus I3C and vehicle control and quantitative Ki-67 labeling index. Lung tissues were processed and the percentage of cells that stained positive for Ki-67 were determined as described in Materials and Methods. Columns, mean; bars, SD; *, $P < 0.05$. D, Western immunoblots of lung tissues. Tissue lysates from whole lung tissues of vehicle-treated mice or microdissected tumors (from NNK or NNK plus I3C treated mice) were prepared as described in Materials and Methods, and equal amounts of protein were loaded onto a 4% to 12% SDS-PAGE followed by immunoblot analysis and chemiluminescence detection. Equal loading of protein was confirmed by stripping the immunoblot and reprobing it for β-actin.

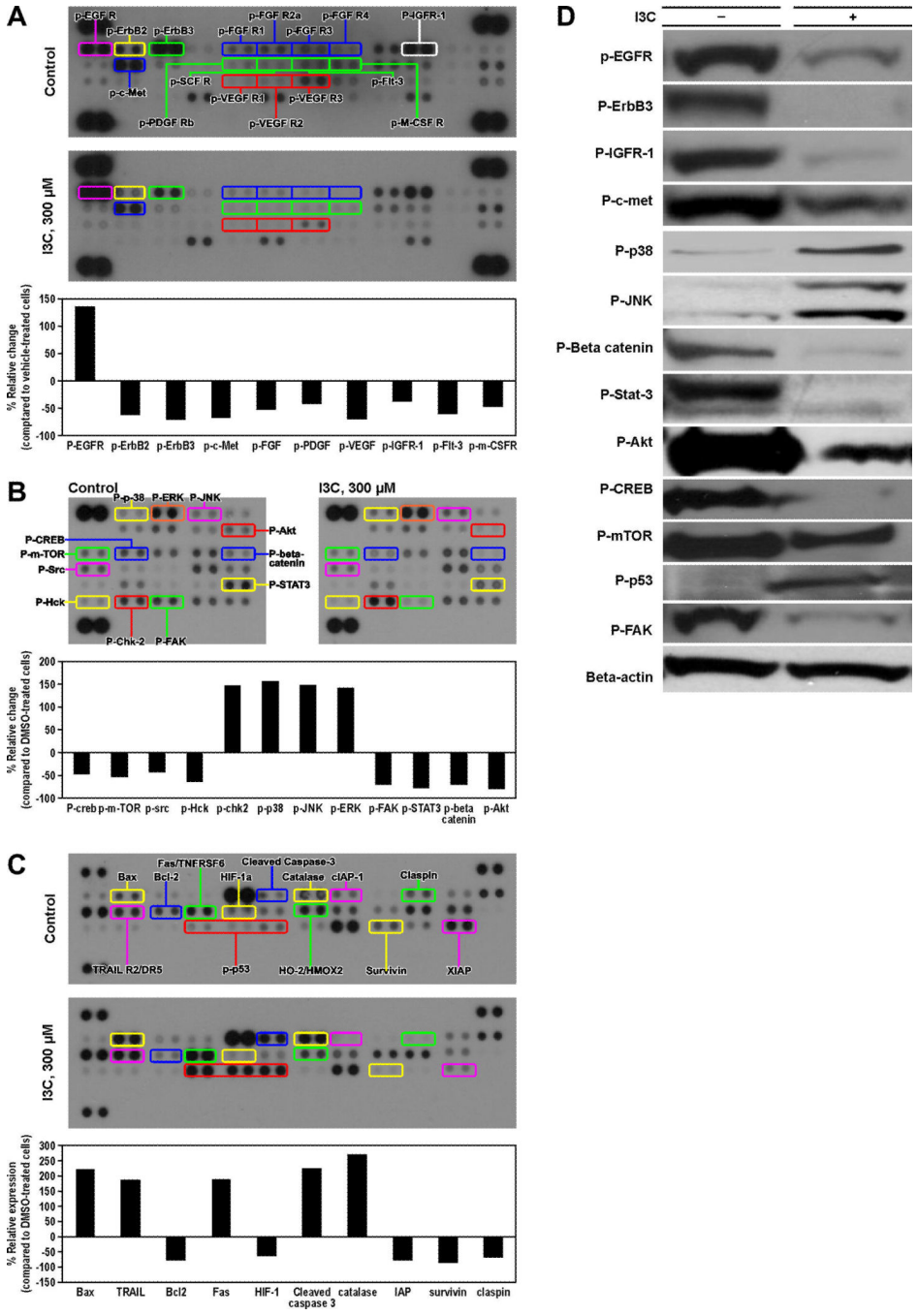

Figure 3.

Effect of I3C on activation of kinases and expression of apoptosis-related proteins in A549 cells. Phosphorylation status of different cancer-related receptor tyrosine kinases (A), intracellular serine/threonine/tyrosine kinase (B) and expression of pro-and anti-apoptotic proteins (C) were compared, using proteome profiler array, in A549 cells treated with DMSO or I3C (300 µM). Quantitative data was generated by analyzing the films using the image analysis software UN-SCAN-IT. The expression of selected proteins was verified by Western immunoblotting using cell lysates prepared from DMSO-treated and I3C-treated (300 µM) A549 cells (D).

Table 1

Effects of I3C on NNK-induced lung tumor incidence and multiplicity in A/J mice[a]

Group	Carcinogen	Chemopreventive agent(dose, μmol/g diet)	Termination of the study	No. of mice	Mean body weight		Lung tumors			
					Initial	At termination	Tumor incidence (%)	Tumors/mouse (mean ± SD)	Reduction in tumor multiplicity (%)	P^b
1	NNK	none	week 27	20	16.3 ± 0.6	22.5 ± 0.5	100	39.9 ± 9.0	-	
2	NNK	none	week 52	20	15.9 ± 0.8	27.9 ± 0.7	100	44.7 ± 6.1	-	
3	NNK	I3C (10)	week 27	20	16.1 ± 0.5	21.8 ± 0.4	100	19.4 ± 4.8	51	< 0.0001
4	NNK	I3C (10)	week 52	20	16.3 ± 0.5	26.9 ± 0.8	100	45.4 ± 5.9	none	-
5	none	none	week 27	10	16.2 ± 0.4	23.9 ± 0.6	20	0.2 ± 0.4	none	
6	none	none	week 52	10	16.4 ± 0.4	28.7 ± 0.4	10	0.1 ± 0.3		
5										

[a] At age 6 weeks, female A/J mice in groups 1–4 were injected (ip) with four doses of NNK (50 mg/kg, in 0.1 ml physiological saline solution, two doses/week). Mice in groups 5 and 6 received the vehicle only. The mice were maintained on AIN-93G diet from age 6 weeks until 1 week after the end of carcinogen treatment, then shifted to AIN-93M diet for the duration of the experiment. Mice in group 3 and group 4 were given I3C in the diet from week 4–27 (post-carcinogen protocol) and week 27–52 (progression protocol), respectively. Mice in groups 1, 3, and 5 were sacrificed at week 27, whereas mice in groups 2, 4, and 6 were sacrificed at week 52.

[b] Compared with Group 1